Chemistry & Biology
Article

Defining Criteria for Oligomannose Immunogens for HIV Using Icosahedral Virus Capsid Scaffolds

Rena D. Astronomo,[1,8] Eiton Kaltgrad,[2,3,9] Andrew K. Udit,[2,3,10] Sheng-Kai Wang,[2,3] Katie J. Doores,[1,4] Cheng-Yuan Huang,[2,3,11] Ralph Pantophlet,[1,12] James C. Paulson,[5,6] Chi-Huey Wong,[2,3] M.G. Finn,[2,3,*] and Dennis R. Burton[1,4,7,*]
[1]Department of Immunology and Microbial Science
[2]Department of Chemistry
[3]The Skaggs Institute for Chemical Biology
The Scripps Research Institute, La Jolla, CA 92037, USA
[4]Ragon Institute of Massachusetts General Hospital, MIT, and Harvard, Boston, MA 02129, USA
[5]Department of Molecular Biology
[6]Department of Chemical Physiology
[7]IAVI Neutralizing Antibody Center
The Scripps Research Institute, La Jolla, CA 92037, USA
[8]Present address: Fred Hutchinson Cancer Research Center, 1100 Fairview Avenue North, Seattle, WA 98109, USA
[9]Present address: Calmune Corporation, 9393 Towne Center Drive, San Diego, CA 92121, USA
[10]Present address: Department of Chemistry, Occidental College, 1600 Campus Road, Los Angeles, CA 90041, USA
[11]Present address: Research Center for Materials Science, Nagoya University, Nagoya 464-15 8602, Japan
[12]Present address: Faculty of Health Sciences, Simon Fraser University, Blusson Hall, 8888 University Drive, Burnaby, BC V5A 1S6, Canada
*Correspondence: mgfinn@scripps.edu (M.G.F.), burton@scripps.edu (D.R.B.)
DOI 10.1016/j.chembiol.2010.03.012

SUMMARY

The broadly neutralizing antibody 2G12 recognizes a conserved cluster of high-mannose glycans on the surface envelope spike of HIV, suggesting that the "glycan shield" defense of the virus can be breached and may, under the right circumstances, serve as a vaccine target. In an attempt to recreate features of the glycan shield semisynthetically, oligomannosides were coupled to surface lysines on the icosahedral capsids of bacteriophage Qβ and cowpea mosaic virus (CPMV). The Qβ glycoconjugates, but not CPMV, presented oligomannose clusters that bind the antibody 2G12 with high affinity. However, antibodies against these 2G12 epitopes were not detected in immunized rabbits. Rather, alternative oligomannose epitopes on the conjugates were immunodominant and elicited high titers of anti-mannose antibodies that do not crossreact with the HIV envelope. The results presented reveal important design considerations for a carbohydrate-based vaccine component for HIV.

INTRODUCTION

A protective vaccine remains widely accepted as the best weapon to combat the spread of HIV-1, but despite tremendous effort a vaccine that induces a neutralizing antibody (Nab) response against a broad range of isolates has yet to be realized (Virgin and Walker, 2010). Difficulties in the elicitation of antibodies (Abs) to conserved regions of the functional envelope spike (Env), responsible for viral infectivity, may largely be attributed to the nature of this target: it is an unstable heterodimeric trimer, composed of glycoproteins gp120 and gp41, in which conserved epitopes are recessed, transiently exposed, or otherwise occluded by highly variable immunodominant loops and a dense glycan shield (Chen et al., 2005; Kwong et al., 1998; Wyatt et al., 1998; Wyatt and Sodroski, 1998). Despite these formidable defenses, a handful of monoclonal broadly neutralizing Abs (bNabs) (Burton et al., 1994; Corti et al., 2010; Trkola et al., 1996; Walker et al., 2009; Zwick et al., 2001) and polyclonal sera (Binley, 2009; Binley et al., 2008; Dhillon et al., 2007; Gray et al., 2009; Li et al., 2009; Stamatatos et al., 2009) from HIV-1-infected individuals suggest that a crossreactive Nab response against HIV-1 can be achieved.

Monoclonal bNabs are potentially valuable tools for the design of effective vaccine components, as their epitopes reveal conserved chinks in the armor of Env that may be exploited. For example, although the "glycan shield" of gp120 is crucial to immune evasion, the bNab 2G12 binds a cluster of oligomannose glycans on the shield, making it a potential vaccine target (Sanders et al., 2002; Scanlan et al., 2002; Trkola et al., 1996). In addition to a broad neutralization profile (Binley et al., 2004; Trkola et al., 1995, 1996), 2G12 protects against infection in non-human primate studies (Hessell et al., 2009; Mascola et al., 2000) and exerts selection pressure on HIV-1 in humans while being well tolerated (Mehandru et al., 2007; Trkola et al., 2005). Thus, the ability to elicit 2G12-like Abs is an important goal for vaccine researchers.

2G12 is specific for terminal Manα1-2Man residues on high-mannose glycans, particularly on the D1 and D3 arms (Calarese et al., 2003, 2005; Scanlan et al., 2002). A variable heavy-domain-exchanged Ab structure creates a compact multivalent binding surface which allows 2G12 to bind its glycan epitope with high affinity (Calarese et al., 2003, 2005). The clustered presentation of the high-mannose glycans on gp120, comprising

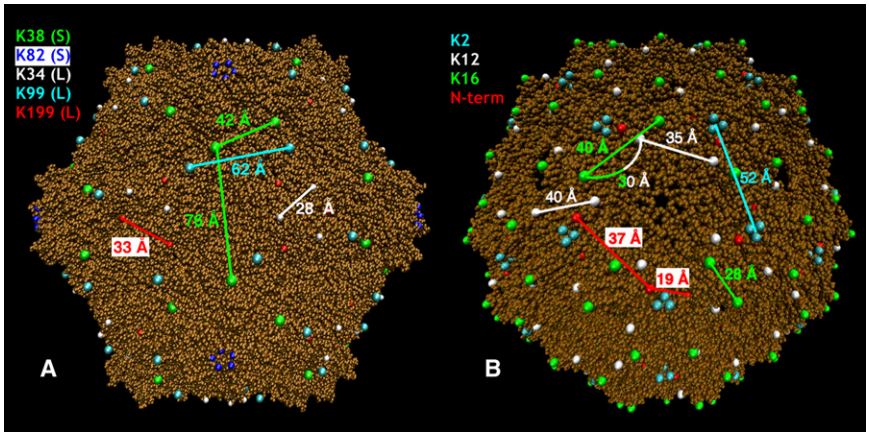

Figure 1. Presentation of Reactive Amino Groups on the Capsid Surfaces of CPMV and Qβ

Capsid structures have been determined by X-ray crystallography.

(A) The CPMV virus surface bears two reactive Lys residues on each of the 60 small (S) subunits and three reactive Lys residues on each of the 60 large (L) subunits; K38 (S) is the most reactive, followed by K99 (L) (Chatterji et al., 2004; Wang et al., 2002).

(B) Qβ displays three accessible Lys residues plus the N-terminal amino group of each of its 180 subunits. The clustered arrangement of K2 at the three-fold axis prevents complete loading of this position. Approximate distances between symmetry-related pairs of reactive amino groups are indicated. These images were made using the coordinates provided by the VIPER database (http://viperdb.scripps.edu) using the program VMD.

this epitope, is thought to form the basis for the immunological discrimination of this epitope as "non-self," although it is composed of "self" glycans. Dense high-mannose clusters are extremely rare among mammalian glycoproteins.

Several studies on the development of a carbohydrate vaccine, using 2G12 as a template, have reinforced the importance of multivalent presentation of oligomannose for mimicking the epitope recognized by 2G12 (Astronomo et al., 2008; Dudkin et al., 2004; Dunlop et al., 2008; Krauss et al., 2007; Li and Wang, 2004; Luallen et al., 2008; Ni et al., 2006; Scanlan et al., 2007; Wang, 2006; Wang et al., 2008). A number of immunogenicity studies have also been carried out, none of which have generated 2G12-like Abs that neutralize HIV-1 (Astronomo et al., 2008; Joyce et al., 2008; Luallen et al., 2008; Ni et al., 2006). Indeed, anti-mannose, gp120-crossreactive Abs are rarely elicited (Luallen et al., 2008). Inadequate mimicry of the oligomannose clusters on gp120 may contribute to this difficulty as well as an inability to elicit domain-exchanged antibodies. Here we describe a novel strategy to create antigenic mimics of high-mannose clusters: synthetic oligomannose ligands, representing the principal epitope of 2G12, are displayed on virus particle scaffolds, using conjugation methods that provide control over the density and conformational flexibility of the attached glycans. This strategy allows for iterative testing of multiple design parameters to fine-tune the presentation of oligomannose.

Two well-characterized icosahedral particles were chosen as our starting platforms: cowpea mosaic virus (CPMV) and the bacteriophage Qβ (Qβ) capsid. The former is a plant virus that infects certain strains of the black-eyed pea plant (*Vigna unguiculata*), and the latter is recombinantly expressed in *Escherichia coli* and self-assembles into a virus-like particle (VLP) around random cellular RNA; neither particle is infectious in mammalian cells. These structures are safe, immunogenic, polyvalent scaffolds for the display of a variety of molecules (Destito et al., 2007; Kaltgrad et al., 2008; Kozlovska et al., 1996; Prasuhn et al., 2007, 2008; Wang et al., 2002), including glycans and peptides (Kaltgrad et al., 2007; Lin et al., 1996; Lomonossoff and Hamilton, 1999; Miermont et al., 2008). Although similar in size, they differ substantially in structural detail, CPMV being composed of 60 large (66 kDa) asymmetric subunits (Lin et al., 1999), whereas Qβ particles are composed of 180 small (14 kDa) subunits that generate a much "smoother" capsid surface (Liljas and Golmohammadi, 1996) (Figure 1). Both particles display reactive amines (lysine residues and the N termini of the Qβ capsid subunits; Kaltgrad et al., 2008; Wang et al., 2002) on their surfaces to which glycans can be attached at distances appropriate for interaction with 2G12. These attachment points differ in number, geometrical arrangement, and conformational flexibility, allowing us to investigate the potential role that such structural variations may play in creating effective glycan shield mimics.

Several glycoconjugates displaying Man_4, Man_8, and Man_9 were created using CPMV and three variants of Qβ which allowed us to examine the impact of density and linker length on overall antigenic mimicry of the glycan shield. The immunogenicity of two constructs is also presented here, providing insight into the impact of epitope heterogeneity on carbohydrate vaccine design for HIV. This study highlights the potential of protein nanoparticles to serve as scaffolds on which to display multiple glycan epitopes for carbohydrate-rich surfaces.

RESULTS AND DISCUSSION

Synthesis and Characterization of CPMV and Qβ Glycoconjugates

The oligomannose compounds **8–10** (Man_4, Man_8, and Man_9, respectively) (Figure 2) are considered to be potential building blocks for the creation of a carbohydrate immunogen to target HIV-1 based on their ability to bind 2G12 with affinities comparable to the naturally derived glycan $GlcNAc_2Man_9$. According to crystallographic and modeling studies, 2G12 likely interacts directly with three high-mannose glycans, at least two of which bind the higher-affinity conventional antigen-combining sites (Calarese et al., 2003). However, it is thought that the conformational and dynamic aspects of the presentation of these glycans are unusual and difficult to reproduce, because the involvement of other neighboring high-mannose glycans on gp120 has been implicated in creating the epitope (Scanlan et al., 2002, 2003).

Using various approaches, an assortment of multivalent carbohydrate antigens have been produced that interact with 2G12 (Calarese et al., 2005; Dudkin et al., 2004; Geng et al., 2004; Krauss et al., 2007; Lee et al., 2004; Li and Wang, 2004;

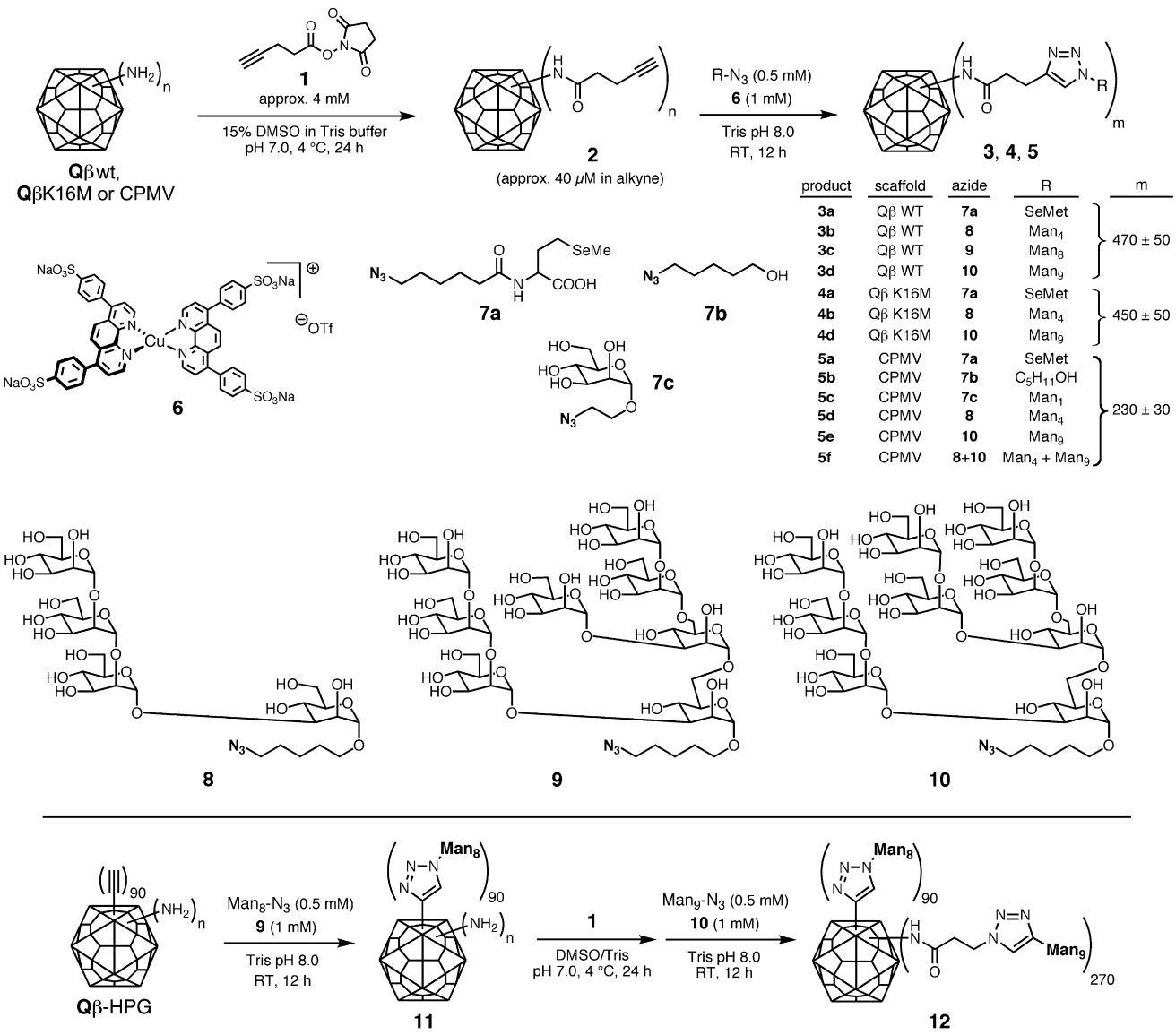

Figure 2. Synthesis of Virus Glycoconjugates

Top: synthesis of Qβwt, QβK16M, and CPMV conjugates. Bottom: stepwise synthesis of QβHPG glycoconjugates QβHPG-Man_8 (**11**) and QβHPG-Man_8/Man_9 (**12**).

Luallen et al., 2008; Ni et al., 2006; Scanlan et al., 2007; Wang, 2006; Wang et al., 2004, 2007, 2008). However, all of these approaches have employed flexible and/or structurally heterogeneous platforms. Virus particles, in contrast, are relatively rigid and structurally homogeneous to atomic resolution. The anticipated importance of oligomannose conformation and clustering therefore prompted us to test virus scaffolds that permit the creation of glycoconjugates presenting oligomannose in different spatial arrangements that are constrained by the positions of the amino acid residues to which attachments are made (Figure 1). In addition to the Qβwt capsid protein shown (Figure 1), two other Qβ variants were prepared: QβK16M, a point mutant in which the most exposed Lys was changed to Met, and QβHPG, an expression variant of QβK16M in which an alkyne-containing unnatural amino acid was incorporated instead of Met at position 16 (Strable et al., 2008). The QβHPG scaffold enabled us to attach different glycans at different positions in a sequential fashion, a capability that improves the overall homogeneity of mixed-glycan conjugates.

High-density glycan display by chemical coupling of the sugars to a scaffold requires a conjugation reaction that is sufficiently strongly driven to overcome unfavorable steric interactions that such crowding may create. In this case, efficient conjugation is particularly important because these oligomannosides are the products of lengthy and technically demanding syntheses. We implemented a two-step strategy, first acylating the surface amino groups with a large excess of alkynyl *N*-hydroxysuccinimide ester **1** (Figure 2). Following purification

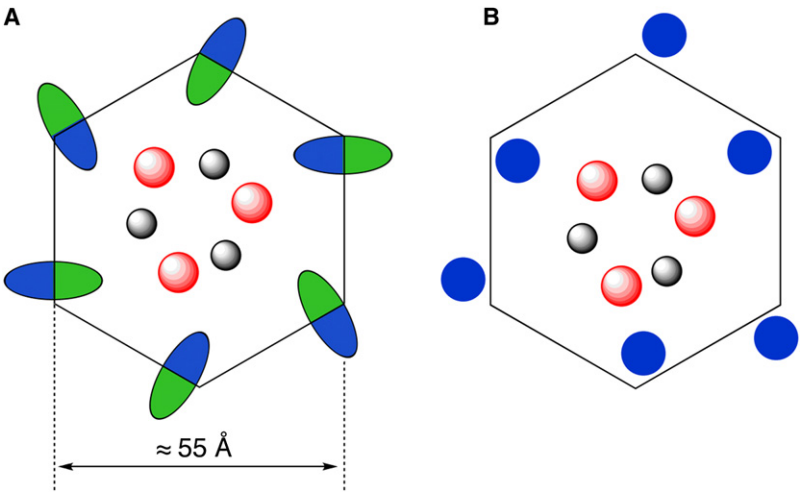

Figure 3. Representations of the Display Patterns around the Three-Fold Symmetry Axis on the Surface of QβwtandQβK16M

(A) Qβwt.

(B) QβK16M.

The colored spheres represent triazole linkages to the following: K12 (blue), K16 (green), K2 (red), and the N terminus (black). Because K12 and K16 are very close to each other (~8 Å apart), it is unlikely that both bear attached glycans in each subunit of the wild-type structure. The oval shapes in (A), therefore, represent a triazole linkage made at one of the two residues (K12 or K16). Based on this model, the overall glycan display patterns for Qβwt and QβK16M glycoconjugates are very similar.

from excess linker, the desired azides were attached with the copper-catalyzed azide-alkyne cycloaddition (CuAAC) reaction (Rostovtsev et al., 2002), enhanced by a ligand known to strongly accelerate the process (Lewis et al., 2004; Sen Gupta et al., 2005). Azidoalkyl linkers are commonly employed in glycan synthesis as precursors to terminal amines and are stable toward extended storage, as are the alkyne groups placed on the protein. The CuAAC "click reaction" allows these stable reactive groups to be employed at low concentrations to achieve reproducibly high loadings.

The resulting constructs **3**, **4**, and **5** (Figure 2), differing in the starting platform (Qβwt, QβK16M, and CPMV, respectively) and, therefore, in the number and geometry of available conjugation points, were characterized by size-exclusion chromatography, polyacrylamide gel electrophoresis, and transmission electron microscopy (see Figure S1 available online). The final conjugates were isolated in 60%–70% yields. The number of triazole-tethered glycans on each particle was estimated by parallel reactions using the selenomethionine azide derivative **7a**, which more closely mimics the hydrophilicity of carbohydrates than dyes (e.g., fluorescein) previously used for this purpose (Figure 2). Reproducible measurements of 230 ± 30 attachments to CPMV, 470 ± 50 to Qβwt VLP, and 450 ± 50 to QβK16M particles were made using inductively coupled plasma optical emission spectroscopy. These values provide an upper limit for the numbers of bulkier glycans attached, because steric crowding will be more pronounced in these cases than for the SeMet label **7a**. CPMV bears fewer reactive amines on its surface than does Qβ, accounting for the lower density of attached glycans (Figure 1). Although the QβK16M has 180 fewer lysine attachment points than the Qβwt capsid, their loading values were very similar, suggesting that the closely spaced K12 and K16 residues (~8 Å apart) were not both derivatized on Qβwt, and that loss of K16 may have allowed the K12 to be fully accessed (Figure 3).

To minimize the length of the linker connecting the scaffold to the glycans, which may impact the antigenicity of resultant conjugates, we expressed the QβK16M mutant construct in an *E. coli* Met auxotroph in the presence of the alkyne-containing amino acid homopropargyl glycine (HPG) in the manner of Tirrell and coworkers (Strable et al., 2008). HPG was incorporated at position 16 with 50% efficiency as determined by mass spectrometry (MS) and CuAAC reaction with SeMet **7a** (Strable et al., 2008) (Figure S2). Conjugation of azide **9** under the same conditions provided conjugate **11** (QβHPG-Man_8) (Figure 2). Conjugate **12** (QβHPG-Man_8/Man_9) was produced by subjecting **11** to another round of elaboration with NHS alkyne **1** and azide **10**. By parallel loading with SeMet **7a**, we estimated 270 ± 30 Man_9 glycans were added to the capsid surface in addition to the 90 Man_8 glycans attached at position 16. MALDI MS analysis of QβHPG-Man_8/Man_9, after dissociation of the particles into their component subunit proteins, also showed only a small amount of nonmannosylated protein, with major components bearing 1–3 oligomannose glycans (Figure S2).

QβHPG-Man_8/Man_9, therefore, displays Man_8 on a shortened tether at the most highly exposed position, with numerous Man_9 glycans distributed over the rest of the surface on the longer conventional linker. We reasoned that this type of mixed particle may be beneficial for mimicking the microheterogeneity found on HIV. The QβHPG scaffold also provided a unique opportunity to study a controlled, mixed conjugate where the position of one of the two glycans is fixed (in this case, Man_8). In contrast, CPMV-Man_4/Man_9 (**5f**) was the product of a single conjugation using a mixture of Man_4 and Man_9 azides, resulting in a random distribution of the two oligosaccharides over the particle surface. The CPMV and Qβ scaffolds thereby provide examples of different arrangements and densities of oligomannose display, whereas the QβHPG scaffold affords the opportunity to investigate what effect a more rigid display format may have on 2G12 binding.

Interaction of Capsid Conjugates with 2G12

The presence of the attached oligomannose ligands was first verified by the observation of rapid aggregation of dilute samples when mixed with the tetravalent mannose-binding lectin concanavalin A (ConA) (Figure S3). A conventional ELISA, in which serial dilutions of 2G12 were allowed to bind antigen coated directly onto wells, was then used to compare the affinity of 2G12 for the capsid conjugates with that of $gp120_{JR-FL}$ (Figure 4A). Qβwt and QβK16M conjugates of Man_4 and Man_9 interacted with 2G12 with nanomolar apparent affinities (~50-fold

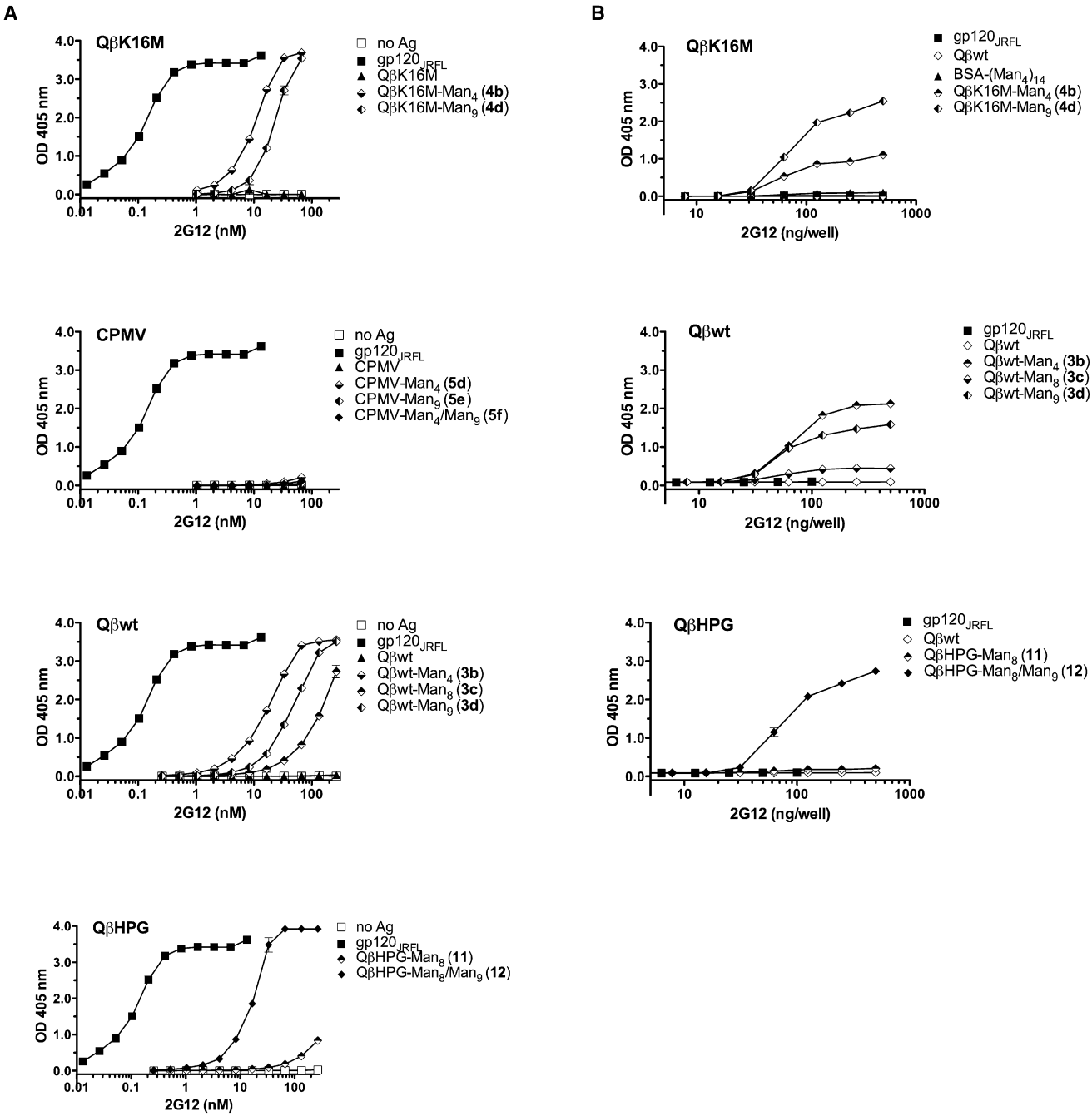

Figure 4. Polyvalent Displays on Icosahedral Virus Capsids Mimic the Glycan Shield

The relative affinities of 2G12 for Qβwt, QβK16M, CPMV, and QβHPG glycoconjugates compared with that of 2G12 for $gp120_{JR\text{-}FL}$ were estimated by a conventional ELISA format (A). Serial dilutions of 2G12 IgG were allowed to bind antigens coated onto ELISA wells. 2G12 was detected with alkaline phosphatase-conjugated anti-human IgG. The relative affinity and number of 2G12 epitope mimics displayed on the surface of QβK16M, Qβwt, and QβHPG were examined in a 2G12 sandwich assay (B). Titrations of 2G12 were coated onto ELISA wells upon which 5 μg/ml solutions of glycoconjugates were captured and then detected by biotinylated 2G12. In these assays, the various glycoconjugates may be compared relative to one another based on both the number of displayed epitope mimics (saturation binding level) and their overall apparent affinity (half-max binding level).
Error bars indicate the standard deviation between duplicate points.

weaker than the cognate antigen gp120 in the best case), ranking them among the best 2G12-binding antigenic mimics described thus far. In contrast, none of the particles bearing lower densities of oligomannose glycans (CPMV conjugates **5d–f** or the lightly loaded QβHPG-Man_8 particle **11**) bound effectively to 2G12. To ensure that the observations for the CPMV conjugates were not an artifact of poor antigen adsorption, CPMV conjugates were independently confirmed to be

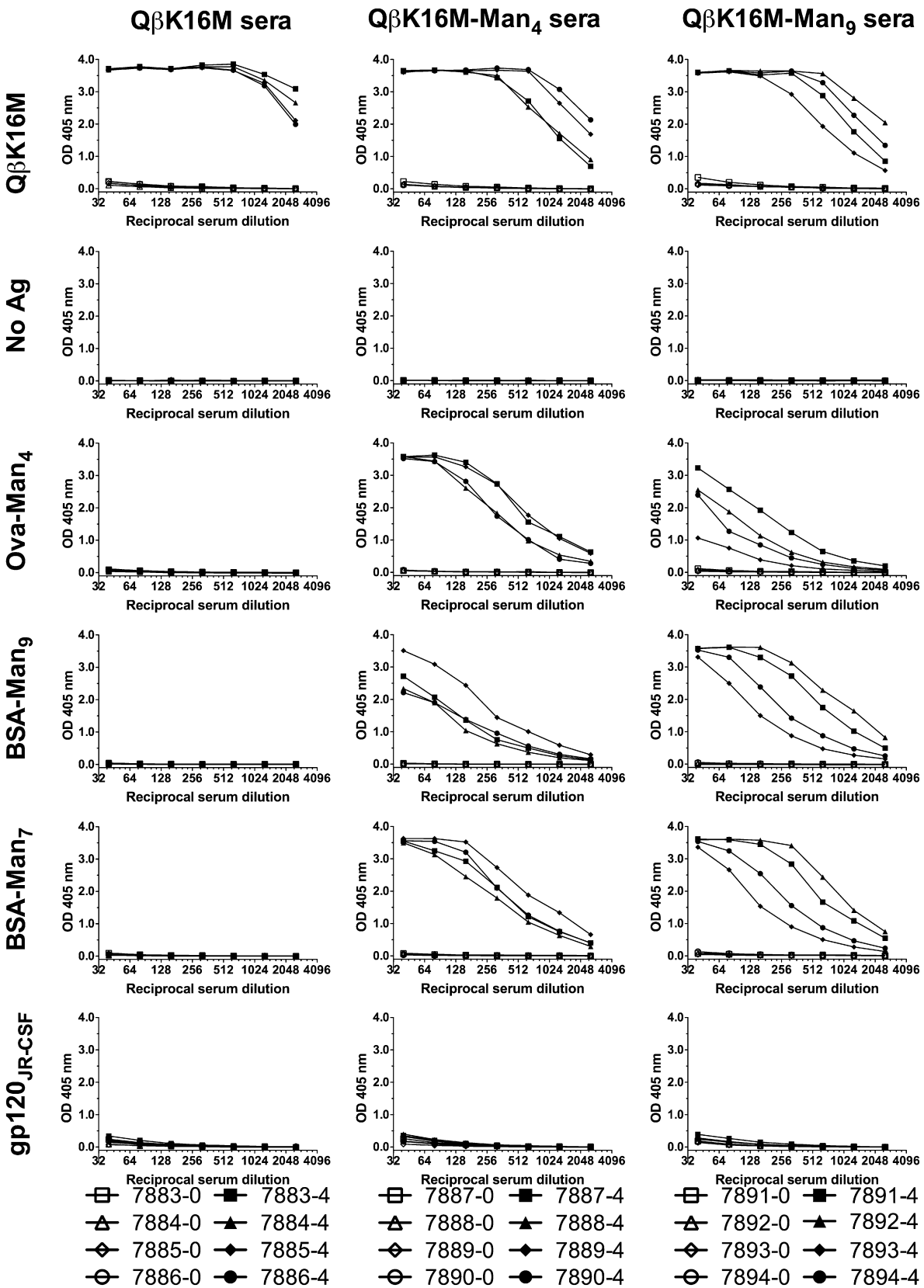
QβK16M sera
QβK16M-Man4 sera
QβK16M-Man9 sera
QβK16M
No Ag
Ova-Man4
BSA-Man9
BSA-Man7
gp120JR-CSF
OD 405 nm
Reciprocal serum dilution
32 64 128 256 512 1024 2048 4096
0.0 1.0 2.0 3.0 4.0
7883-0 7883-4
7884-0 7884-4
7885-0 7885-4
7886-0 7886-4
7887-0 7887-4
7888-0 7888-4
7889-0 7889-4
7890-0 7890-4
7891-0 7891-4
7892-0 7892-4
7893-0 7893-4
7894-0 7894-4

deposited onto ELISA wells in quantities comparable to naked CPMV particles by detection with anti-CPMV polyclonal Ab (data not shown).

Qβwt-Man_9 (**3d**), QβK16M-Man_9 (**4d**), and especially Qβwt-Man_8 (**3c**) showed weaker binding than the corresponding Qβ conjugates of Man_4 (**3b** and **4b**), which was unexpected because the larger oligomannosides are structurally more similar to the high-mannose glycans comprising the epitope of 2G12 on HIV (Figure 4A). This suggested that the highly glycosylated nature of these conjugates may have impeded their adsorption onto the plastic wells, more so for those displaying the larger glycans. Thus, this assay potentially underestimates the affinities of 2G12 for these VLP glycoconjugates, especially for the high-density Man_8 and Man_9 conjugates.

To address this possibility, a modified 2G12 sandwich ELISA was employed which takes into account both the affinity and the number of 2G12-like glycan epitopes (Figure 4B). Virus conjugates were captured onto ELISA wells by titrated amounts of immobilized 2G12. The antigens were then detected with a saturating concentration of biotinylated 2G12. A previously described synthetic antigen for 2G12, BSA-$(Man_4)_{14}$, and $gp120_{JR\text{-}FL}$ were included for comparison (Astronomo et al., 2008). Only one high-affinity epitope is present on wild-type gp120 (despite the presence of ~13 high-mannose glycans on its surface) (Cutalo et al., 2004), giving rise to the observed lack of biotinylated 2G12 binding to gp120 in this assay format (Figure 4B). Likewise, multiple 2G12-like epitopes are not evident for BSA-$(Man_4)_{14}$. In contrast, the Qβwt, QβK16M, and QβHPG-Man_8/Man_9 conjugates display multiple high-affinity binding sites, as shown in Figure 4B. Here, QβK16M-Man_9 (**4d**) proved to be superior to its Man_4 analog; on wild-type Qβ, the difference was less pronounced in favor of Man_4. Qβwt-Man_8 (**3c**) was much less effective than both Man_4 and Man_9 conjugates.

The contrasting performance of CPMV and Qβ is striking and suggests that the manner of glycan display plays a critical role in their recognition by 2G12; for example, one may surmise that the arrangement of glycans on the CPMV scaffold does not adequately mimic that of gp120. Lysines K38 and K99 are the most reactive on the CPMV surface, accounting for approximately 120 displayed glycans at distances shown in Figure 1A. The remaining ~110 glycans would be distributed among the other sites, with poor conjugation efficiency on K82 because of its passivation in a 5-fold salt-bridge interaction with neighboring D81 residues (Wang et al., 2002). The overall result is expected to be a surface decorated with pairs or trios of glycans at appropriate distances from one another to interact with 2G12. However, additional neighboring glycans, which may play a role in buttressing these epitopes, would be rare (Figure 1A). Qβwt or QβK16M should provide appropriately spaced glycans closely surrounded by additional glycans restricting their conformational flexibility, enhancing their affinity for 2G12 (Figure 1B). The similar level of antigenic mimicry observed, based on 2G12 binding, between analogous QβK16M and Qβwt conjugates corresponds well with the grossly similar glycan arrangements we predicted for these scaffolds.

More precisely controlled conjugation (only at position 16 of Qβ) of Man_8 was accomplished on a shorter tether (directly to the amino acid side chain) by using QβHPG to give QβHPG-Man_8 (**11**). Given the poor recognition of Qβwt-Man_8 (**3c**) by 2G12, and the lower loading of Man_8 on QβHPG (~90 glycans), it was not surprising to find QβHPG-Man_8 to be a poor antigen for 2G12 (Figure 4). However, when the rest of the platform was "filled in" with Man_9 residues, the combined display of Man_8 and Man_9 gave rise to the most effective glycoconjugate antigen: QβHPG-Man_8/Man_9 (**12**) bound 2G12 as well as the best K16M and wild-type conjugates despite having approximately 25% fewer glycans (Figure 4). Such a result suggests that shorter linkers, in addition to a threshold density of attachment, may improve the presentation of high-mannose glycans for 2G12 binding and, consequently, antigenic mimicry of the gp120 glycan shield. The shorter linker may decrease the overall flexibility of the glycan epitopes and thereby reduce the entropic penalty associated with 2G12 binding. The synthesis and binding studies of the QβHPG conjugates presented here constitute the first exploration to our knowledge, albeit preliminary in nature, of the impact of linker length and controlled combinatorial display.

Immunogenicity of QβK16M Glycoconjugates

Because the QβK16M-Man_4 and QβK16M-Man_9 conjugates displayed multiple high-affinity epitopes for 2G12 with potentially less heterogeneity compared with the corresponding Qβwt conjugates, these constructs were tested for their immunogenic properties in rabbits. The rabbit IgG response against QβK16M-Man_4 and QβK16M-Man_9 peaked after the second immunization and showed no further boosting effects from the third and fourth immunizations. Preimmune and fourth-bleed sera were titrated against the naked carrier protein QβK16M and a series of glycoconjugates that utilized a different linker (Figure S4) to better measure the overall Ab response against the carbohydrate portion of the displayed ligands (Figure 5). Overall, the anti-mannose Abs elicited against QβK16M-Man_4 reacted most effectively with Man_4, followed very closely by Man_7, the D1/D2 biantennary glycan. In contrast, the serum Abs elicited by QβK16M-Man_9 reacted most effectively with Man_9 and nearly as well with Man_7, but only moderately with Man_4. Similar trends were observed when IgG titers against analogous CPMV conjugates were measured (Table S1). These results suggest that immunization with QβK16M-Man_4 or QβK16M-Man_9 elicits strong anti-mannose responses with distinct Ab specificities. The polyclonal Ab response to the Man_4 glycoconjugate appears to be tailored toward recognition of the D1 structure in simpler contexts (i.e., Man_4 and Man_7). The response to the Man_9 glycoconjugate reacts better with branched structures that include more structural elements (arms) in common with the glycan immunogen. This may reflect the presence of Abs against

Figure 5. Representative Immunogenicity Profiles for QβK16M-Man_4 and QβK16M-Man_9

Serum Ab titers from rabbits immunized with QβK16M virus glycoconjugates or naked QβK16M particles. Symbol keys below each panel of graphs indicate rabbit ID numbers; open symbols correspond to preimmune sera and filled symbols correspond to fourth-bleed immune sera. Antigens are denoted on the left of each graph. Man_7 corresponds to the D1/D2 motif, that is, Manα1-2Manα1-2Manα1-3Man(Manα1-2Manα1-3Manα1-6)Man.

branched structures in Man_9 and/or Abs against individual arms of Man_9.

The reactivity of anti-mannose serum Abs with HIV-1 gp120 glycans was initially assessed with recombinant $gp120_{JR-FL}$, which corresponds to a primary HIV-1 isolate that is potently neutralized by 2G12 (Binley et al., 2004). No reactivity was observed above background levels with $gp120_{JR-FL}$ or with two additional recombinant gp120s: one derived from a virus isolate, JR-CSF, sensitive to 2G12 neutralization, and the other, YU2, neutralized poorly by 2G12 (Binley et al., 2004; Trkola et al., 1996). These two gp120 antigens were chosen because they present different degrees of high-mannose glycosylation, the $gp120_{YU2}$ presumably having less high-mannose clustering and the $gp120_{JR-CSF}$ having more high-mannose clustering. Pseudovirus neutralization assays also confirmed that the anti-mannose Abs elicited by both of the Qβ glycoconjugates could not interact with the glycan shield of HIV either in the context of monomeric gp120 or the envelope spike (Table S1). These results were especially striking for the QβK16M-Man_9 group, given the high titers of Man_9-reactive Abs observed. The immune sera also did not react with two other glycoproteins known to display lower densities of high-mannose glycans (Table S1) (Iacob et al., 2008; Joao and Dwek, 1993).

Only moderate reactivity was observed with CPMV control particles bearing hydroxypentyl (from **5b**) or single mannose (from **5c**) groups, suggesting that the majority of Abs were elicited against the oligomannose structures rather than the linker motifs, although the possibility of some linker dependency cannot be excluded. Taken together, these results suggest that the Qβ conjugates induce anti-mannose antibodies that recognize epitopes displayed on the synthetic neoglycoconjugates, but not on the mammalian and viral glycoproteins tested here. In order to further probe the fine specificities of the antibody responses to these capsid glycoconjugates, the immune serum IgGs were also analyzed on the printed glycan array created by the Consortium for Functional Glycomics.

The serum reactivity profiles indicate that both Qβ glycoconjugates elicit IgGs that strongly recognize synthetic fragments of high-mannose oligosaccharides terminating in Manα1→2Man and/or containing Manα1→3Man motifs (Figure 6). In contrast, no substantial binding was observed with the naturally derived *N*-linked high-mannose glycans, including $GlcNAc_2Man_8$ (193) and $GlcNAc_2Man_9$ (194) (Figure 6). These results are consistent with the ELISA results presented above, and suggest that the antibody specificities elicited by both Qβ glycoconjugates discriminate between truncated synthetic oligomannose and full-length *N*-linked high-mannose glycans containing the chitobiose core.

Dissection of the antibody response to Qβ-displayed Man_4 versus Man_9 was also intriguing. The QβK16M-Man_9 response was much more specific, showing consistently high titers in the sera of all animals against only Man_9 (314 on the array). The specificity profiles of these rabbits against the other high-mannose sugars varied significantly. In contrast, the individual profiles for the QβK16M-Man_4 group were very similar to one another and to the BSA-$(Man_4)_{14}$ immune serum profiles described previously (Astronomo et al., 2008) for a variety of high-mannose fragments. Aside from the natural glycans, all immune sera in the Man_9 group generally reacted poorly to α-D-Man (9) and oligomannosides corresponding to internal structures shared by Man_9 and $(GlcNAc)_2Man_9$, namely 195, 311, and 312 (Figure 6B). These results suggest that immunization with QβK16M-Man_9 elicits Ab specificities geared predominantly toward the terminal Manα1→2Man motifs of branched high-mannose glycans and not toward the internal motifs and linker. Immune sera 7891 and 7893, especially, exhibited preferential recognition of Man_9 (314) over all other related synthetic derivatives including Man_8 (313), which differs from Man_9 only by the loss of the terminal D2 mannose residue (Figure 6). Overall, these results suggest that the immune system can discriminate between the terminal structures of synthetic Man_9 and $GlcNAc_2Man_9$ through differences in presentation and/or conformation. Accordingly, synthetic Man_9 seems to adopt structural presentations and/or conformations in addition to those recognized by 2G12.

We next used competition ELISAs to determine whether the rabbit Abs raised against our Qβ conjugates recognized the same synthetic oligomannose epitopes as 2G12. Preincubation of immune sera with excess naked Qβ particles successfully dampened reactivity to the Qβ scaffold (Figure 7A). To assess epitope overlap, the binding of these serum IgG samples to the Qβ glycoconjugates was tested after exposure of the particles to serially diluted 2G12, but no inhibition by 2G12 was observed (Figure 7B). Similarly, 2G12 binding to the glycoconjugates was also unaffected by the presence of the immune sera (Figure 7C). These competition results suggest the existence of epitope heterogeneity on the Qβ glycoconjugates, and immunization with these constructs elicits anti-glycan Ab responses primarily against epitopes (i.e., structural presentations/conformations) different from those recognized by 2G12.

The striking inability of antibodies elicited against Qβ-high-mannose conjugates to bind $GlcNAc_2Man_9$ suggests that the presentation of the glycan might be influenced by its manner of connection to the scaffold or the nature of that scaffold. Perhaps the difference in flexibility between the linkers is responsible (the synthetic oligomannose glycans being tethered to the carrier protein particle by flexible polycarbon chains compared with the shorter direct connection with the chitobiose core). Furthermore, or alternatively, the extensive internal hydrogen-bonding network that maintains the overall topology of $GlcNAc_2Man_9$ (Woods et al., 1998) may not be preserved in the absence of the chitobiose core (Shenoy et al., 2002). Both of these scenarios would lead to differential access to various mannosyl faces as potential epitopes, especially if the glycans (particularly the Manα1→2Man motifs) are not closely spaced together. However, it should be noted that immunization with synthetic $GlcNAc_2Man_9$-based mimitopes in an attempt to elicit 2G12-like antibodies has also failed to elicit convincing gp120 cross-reactive Ab responses (Joyce et al., 2008; Ni et al., 2006).

Our efforts to limit the flexibility of the displayed glycans by using carriers with densely clustered attachment sites and by making use of the branching of Man_9 itself did not give rise to 2G12-like antibody responses. It would therefore seem that the synthetic clusters on our conjugates are all too reminiscent of the natural glycan shield, in that the high-affinity 2G12 binding sites are poorly immunogenic in comparison with alternative epitopes not recognized by 2G12 (i.e., presumably less clustered glycans), and no evidence of the elicitation of domain-exchanged antibodies was gained. This suggests that altering the presentation of glycans on Qβ to limit the display of inadequately

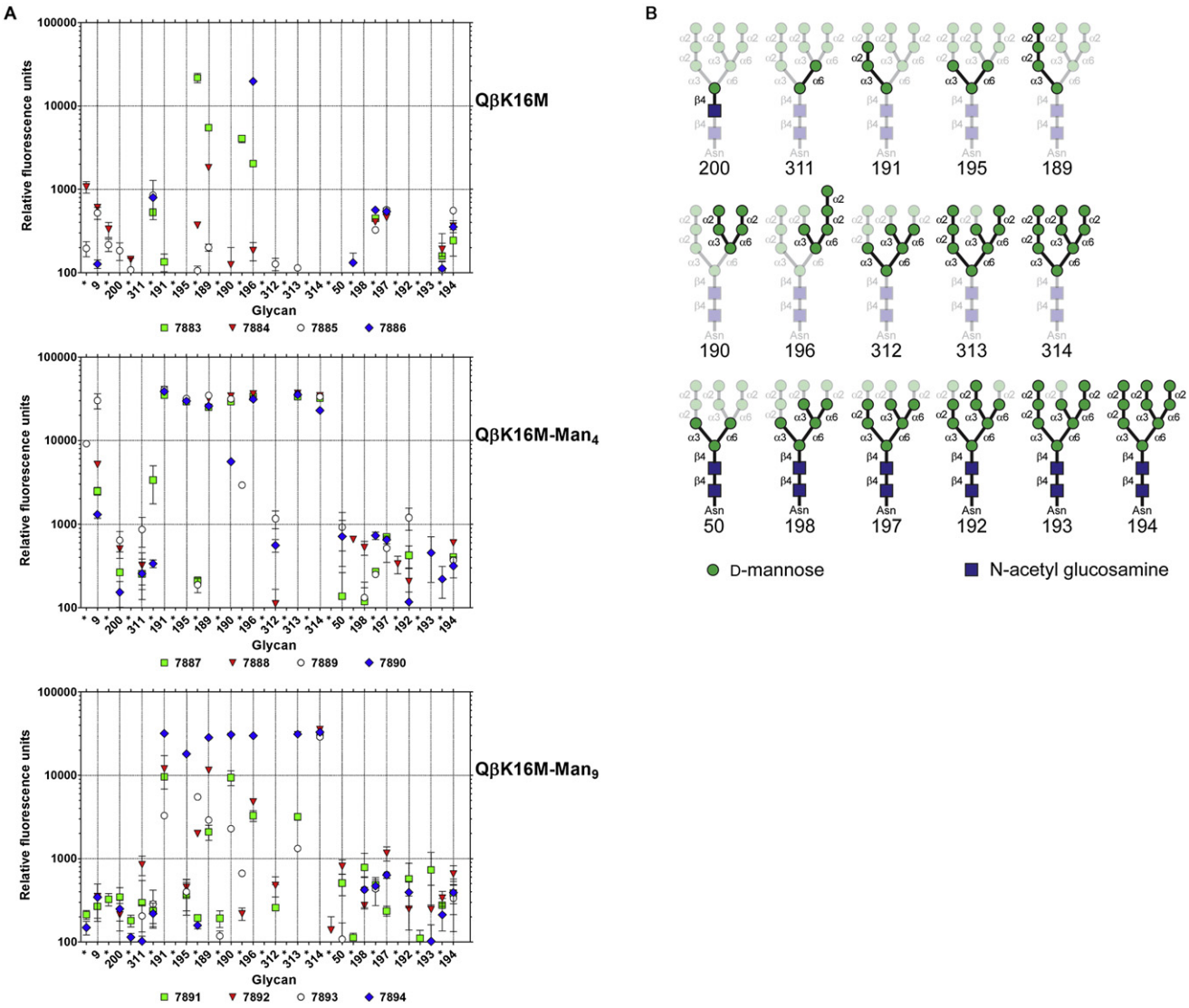

Figure 6. Glycan Array Analysis of the Anti-Mannose Specificities Elicited by QβK16M Glycoconjugates

(A) Serum IgG recognition of α-D-mannose and various synthetic and naturally derived oligomannosides present on printed glycan array V3.0. Binding of prebleed and final-bleed sera, diluted 1:200, to oligomannose glycans as measured by fluorescence (y axis). Individual glycans assayed are referenced by the glycan ID numbers on the printed array (x axis). Preimmune serum data corresponding to a given sugar are plotted above the asterisks preceding each glycan ID number, whereas immune serum data for a given glycan are plotted above the denoted glycan ID number. Each symbol corresponds to a single rabbit in the QβK16M, QβK16M-Man_4, or QβK16M-Man_9 group. The average over four replicates and the SEM for selected glycans are shown.

(B) Symbolic representations of the oligosaccharides corresponding to the glycan ID numbers in (A) shown in the context of $Man_9(GlcNAc)_2$. Note that glycan 9 is not depicted, as it represents the monosaccharide α-D-mannose.

clustered glycans and, consequently, the unwanted formation of highly immunogenic neo-epitopes, may be required to generate 2G12-like Ab specificities. In addition, strategies to overcome possible tolerance mechanisms, which may suppress B cells specific for the termini of natural high-mannose glycans, warrant investigation as well as presentations that might specifically favor eliciting domain-exchanged antibodies.

SIGNIFICANCE

Multiple strategies have been used to create carbohydrate-based immunogens to target the HIV-1 glycan shield, but minimal success has been reported (Dudkin et al., 2004; Geng et al., 2004; Joyce et al., 2008; Krauss et al., 2007; Li and Wang, 2004; Luallen et al., 2008; Ni et al., 2006; Wang et al., 2004, 2007). Thus, there is much yet to learn about how to elicit 2G12-like, end-binding, Manα1→2Man-specific antibodies that recognize these motifs on HIV but not on "self" tissues. Virus-like particles have long been recognized as promising carriers for immunization because of their immunogenicity, a consequence of their size and regular arrangement of component proteins (Wang et al., 2002). Less appreciated has been the opportunity they offer—by virtue of their participation in well-defined and

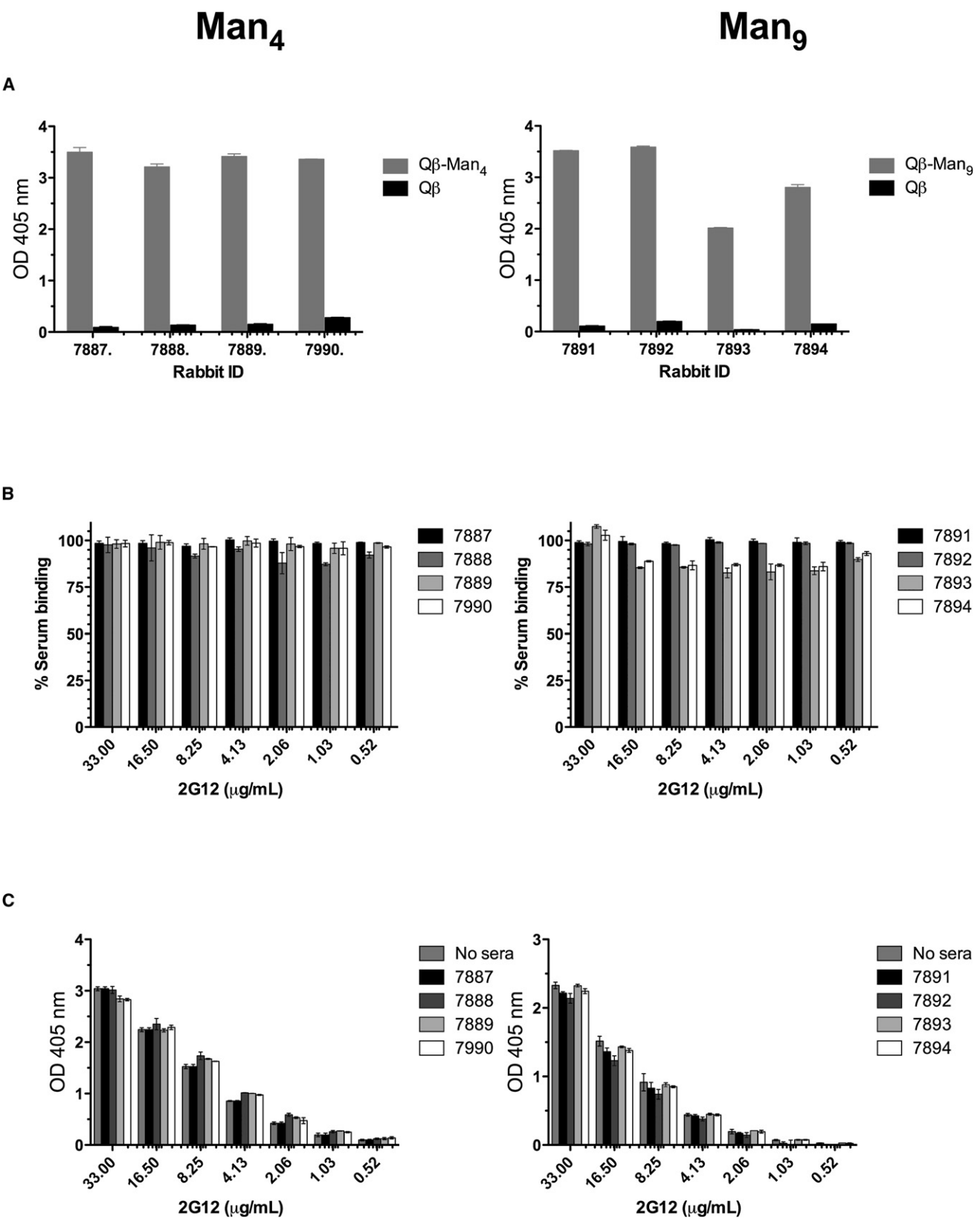
Man4
Man9
A
OD 405 nm
Qβ-Man4
Qβ
7887.
7888.
7889.
7990.
Rabbit ID
Qβ-Man9
7891
7892
7893
7894
B
% Serum binding
7887
7888
7889
7990
7891
7892
7893
7894
33.00
16.50
8.25
4.13
2.06
1.03
0.52
2G12 (μg/mL)
C
No sera

robust chemistry, their relatively rigid structures, and knowledge of these structures at atomic resolution—to test previously unapproachable design aspects of tailored antigens. For carbohydrates, which are typically poorly immunogenic, such details of presentation are crucial and likely amenable to optimization.

Immunization with QβK16M-Man$_4$ and QβK16M-Man$_9$ provided novel insights into the nature of this challenge. Despite the presentation of multiple oligomannose clusters that structurally mimic the HIV glycan shield, as judged by their high affinity for 2G12, the Ab responses in the immunized animals were directed toward alternative epitopes, presumably associated with glycans separate from these clusters. This immunological discrimination may stem from differences in presentation and/or conformation between truncated oligomannose tethered by a synthetic linker and Asn-(GlcNAc)$_2$-linked high-mannose glycans. These studies strongly suggest that refinements to improve epitope homogeneity and/or the immunogenicity of 2G12 epitope mimics on Qβ scaffolds may be crucial for directing the immune system to recognize the glycan shield of infectious HIV and thus lead to effective vaccine immunogens.

EXPERIMENTAL PROCEDURES

Oligomannose-Azide Ligands

Detailed descriptions of the syntheses (except for Man$_7$; see Supplemental Information) and characterization of these glycans have been published previously (Calarese et al., 2005; Lee et al., 2004).

Synthesis of Glycoconjugates

CPMV-carbohydrate conjugates **5a**–**5f**: CPMV-alkyne **2** derived from the reaction of CPMV with NHS ester **1** was pelleted by ultracentrifugation and resuspended in degassed 0.1 M Tris buffer (pH 8.0) in a nitrogen-filled glove box. This solution (2 mg/ml, 21 μM in protein, 0.35 μM in particles) was treated with **7a**–**7c**, **8**, **10**, or a 1:1 mixture of **8** and **10** (0.3 mM), in each case mixed with the components of Cu complex **6** (1 mM CuOTf + 2 mM sulfonated bathophenthroline ligand), in degassed 0.1 M Tris buffer (pH 8.0), all under an inert atmosphere. Gentle agitation on a slow rotor for 12–18 hr under nitrogen was followed by purification of the virus-triazole conjugates as described above. All Qβ-carbohydrate conjugates were prepared in analogous fashion, using a VLP concentration of 2 mg/ml (140 μM in protein subunits, 0.78 μM in VLPs) and glycan-azide concentration of 0.3 mM. Note that we now recommend a more convenient benchtop procedure involving a different Cu-binding ligand for bioconjugation reactions such as these (Hong et al., 2009).

2G12 ELISA

Two assay formats were employed to measure binding of 2G12 to glycoconjugate antigens. Ab binding was visualized with *p*-nitrophenol phosphate substrate (Sigma), and development was monitored at 405 nm.

Conventional Assay

Flat-bottomed microtiter plate wells (Costar type 3690; Corning) were coated with 250 ng of antigen in PBS overnight at 4°C. Subsequent steps were done at room temperature. The plates were washed with PBS/0.05% Tween 20 (PBS-T) and then blocked with 3% BSA (100 μl/well) for 1 hr. The wells were then emptied and serially diluted 2G12 (Polymun Scientific) in 1% BSA/0.02% Tween 20/PBS (PBS-BT) was allowed to bind antigen for 2 hr at RT followed by another series of washes. Antibody binding was probed with alkaline phosphatase-conjugated goat anti-human IgG, Fc fragment-specific secondary (Jackson ImmunoResearch Laboratories) diluted 1:1000 in PBS-BT (1 hr). Unbound secondary Ab was then washed and plates were developed as described above.

Capture Assay

General assay conditions, procedures, and buffer solutions were as described above, except as follows. Serial dilutions of 2G12 IgG were coated onto ELISA wells overnight, washed, and blocked. Antigens (5 μg/ml) were then captured for 2 hr at RT followed by another series of washes and probed with 20 μg/ml biotinylated 2G12 IgG (BT-2G12, saturating conditions) for an additional 2 hr. Detection of BT-2G12 was achieved by incubation with 1:500 diluted streptavidin-AP (Vector Labs) for 1 hr.

Serum Titration ELISA

Serum binding to various antigens was measured using similar conditions as described above (conventional ELISA) except as follows. ELISA plate wells were coated with 250 ng of antigen (or 2 μg of ribonuclease B or 500 ng of OVA-Man$_4$, BSA-Man$_7$, or BSA-Man$_9$). Wells were blocked with 5% nonfat milk blocking buffer (5% nonfat milk, 0.05% Tween 20 in PBS). For all ELISAs, serial dilutions of sera (in 1% milk, 0.02% Tween 20 in PBS, or 5% milk) were allowed to bind antigen for 2 hr prior to washing. Ab binding was detected with either 1:1000 diluted alkaline phosphatase-conjugated goat anti-rabbit IgG F(ab′)$_2$ Ab (Pierce) to detect all Ab isotypes or 1:1000 diluted alkaline phosphatase-conjugated goat anti-rabbit IgG Fcγ-specific Ab (Jackson ImmunoResearch Laboratories).

Serum Competition with 2G12

QβK16M-Man$_4$ and QβK16M-Man$_9$ sera from the fourth bleeds were diluted to 1:100 and preincubated with Qβwt particles (300 μg) in Eppendorf tubes (360 μl total volume/tube) which were rotated end over end overnight at 4°C in order to preabsorb Abs against the virus scaffold. These samples were then further diluted to 1:350 in 5% nonfat milk, 0.02% Tween 20 in PBS. ELISA wells were coated with Qβwt-Man$_4$ and Qβwt-Man$_9$ and blocked as described above. Serial dilutions of 2G12 (Polymun Scientific) were added to antigen-coated wells (25 μl) and incubated for 1 hr prior to the addition of 25 μl of sera (1:700 final dilution). After 2 hr, rabbit IgG was detected as described above. 2G12 IgG was detected in the same way as above using alkaline phosphatase-conjugated goat anti-human IgG, Fcγ-specific Ab (Jackson ImmunoResearch Laboratories). Minor crossreactivity between anti-human IgG and rabbit Abs was subtracted from the 2G12 binding curves.

Glycan Microarray Analysis

Preimmune and immune (fourth bleed) sera from rabbits immunized with QβK16M, QβK16M-Man$_4$, and QβK16M-Man$_9$ were screened on printed glycan array version 3.0 from the Consortium for Functional Glycomics (CFG) as described previously (Blixt et al., 2004; Astronomo et al., 2008). Complete glycan array data sets may be found at http://www.functionalglycomics.org in the CFG data archive under "cfg_rRequest_923."

SUPPLEMENTAL INFORMATION

Supplemental Information includes Supplemental Experimental Procedures, four figures, and one table and can be found with this article online at doi:10.1016/j.chembiol.2010.03.012.

Figure 7. Recognition of Distinct Carbohydrate Epitopes by 2G12 and Serum Anti-Mannose IgG

ELISA binding assays to Qβwt-Man$_4$ (left panels) and Qβwt-Man$_9$ (right panels) glycoconjugates were performed with 1:700 diluted sera from the fourth bleed which were preincubated with naked Qβwt particles. Sera from QβK16M-Man$_4$ and QβK16M-Man$_9$ immunizations were assayed on Qβwt-Man$_4$ and Qβwt-Man$_9$, respectively.

(A) Binding of immune serum IgG to Qβwt glycoconjugates compared with underivatized Qβwt particles.

(B) Residual binding (%) of immune serum IgG to Qβwt glycoconjugates in the presence of serially diluted 2G12.

(C) Binding of serially diluted 2G12 to Qβwt glycoconjugates in the presence and absence of QβK16M-Man$_4$ and QβK16M-Man$_9$ sera. Error bars indicate the standard deviation between duplicate points. Representative data are shown from repeat experiments.

ACKNOWLEDGMENTS

We greatly appreciate the gift of 2G12 from Gabriela Stiegler and Hermann Katinger (Polymun Scientific, Vienna, Austria; University of Natural Resources and Applied Life Sciences, Vienna, Austria) and the glycan array resources provided by Core D and Core H of the CFG funded by NIGMS (GM062116). We also thank Michael Huber for critical reading of the manuscript. The work was supported by the Natural Sciences and Engineering Research Council of Canada (to R.D.A.), the Canadian Institutes of Health Research (to A.K.U.), the Neutralizing Antibody Consortium of the International AIDS Vaccine Initiative (to D.R.B.), the Skaggs Institute for Chemical Biology (to M.G.F.), the National Institutes of Health (AI33292 and AI060425 to D.R.B. and GM083658 to M.G.F.), and the Ragon Institute (to D.R.B. and K.J.D.).

Received: February 25, 2009
Revised: March 24, 2010
Accepted: March 25, 2010
Published: April 22, 2010

REFERENCES

Astronomo, R.D., Lee, H.K., Scanlan, C.N., Pantophlet, R., Huang, C.Y., Wilson, I.A., Blixt, O., Dwek, R.A., Wong, C.H., and Burton, D.R. (2008). A glycoconjugate antigen based on the recognition motif of a broadly neutralizing human immunodeficiency virus antibody, 2G12, is immunogenic but elicits antibodies unable to bind to the self glycans of gp120. J. Virol. *82*, 6359–6368.

Binley, J. (2009). Specificities of broadly neutralizing anti-HIV-1 sera. Curr. Opin. HIV AIDS *4*, 364–372.

Binley, J.M., Wrin, T., Korber, B., Zwick, M.B., Wang, M., Chappey, C., Stiegler, G., Kunert, R., Zolla-Pazner, S., Katinger, H., et al. (2004). Comprehensive cross-clade neutralization analysis of a panel of anti-human immunodeficiency virus type 1 monoclonal antibodies. J. Virol. *78*, 13232–13252.

Binley, J.M., Lybarger, E.A., Crooks, E.T., Seaman, M.S., Gray, E., Davis, K.L., Decker, J.M., Wycuff, D., Harris, L., Hawkins, N., et al. (2008). Profiling the specificity of neutralizing antibodies in a large panel of plasmas from patients chronically infected with human immunodeficiency virus type 1 subtypes B and C. J. Virol. *82*, 11651–11668.

Blixt, O., Head, S., Mondala, T., Scanlan, C., Huflejt, M.E., Alvarez, R., Bryan, M.C., Fazio, F., Calarese, D., Stevens, J., et al. (2004). Printed covalent glycan array for ligand profiling of diverse glycan binding proteins. Proc. Natl. Acad. Sci. USA *101*, 17033–17038.

Burton, D.R., Pyati, J., Koduri, R., Sharp, S.J., Thornton, G.B., Parren, P.W., Sawyer, L.S., Hendry, R.M., Dunlop, N., Nara, P.L., et al. (1994). Efficient neutralization of primary isolates of HIV-1 by a recombinant human monoclonal antibody. Science *266*, 1024–1027.

Calarese, D.A., Scanlan, C.N., Zwick, M.B., Deechongkit, S., Mimura, Y., Kunert, R., Zhu, P., Wormald, M.R., Stanfield, R.L., Roux, K.H., et al. (2003). Antibody domain exchange is an immunological solution to carbohydrate cluster recognition. Science *300*, 2065–2071.

Calarese, D.A., Lee, H.K., Huang, C.Y., Best, M.D., Astronomo, R.D., Stanfield, R.L., Katinger, H., Burton, D.R., Wong, C.H., and Wilson, I.A. (2005). Dissection of the carbohydrate specificity of the broadly neutralizing anti-HIV-1 antibody 2G12. Proc. Natl. Acad. Sci. USA *102*, 13372–13377.

Chatterji, A., Ochoa, W.F., Paine, M., Ratna, B.R., Johnson, J.E., and Lin, T. (2004). New addresses on an addressable virus nanoblock: uniquely reactive Lys residues on cowpea mosaic virus. Chem. Biol. *11*, 855–863.

Chen, B., Vogan, E.M., Gong, H., Skehel, J.J., Wiley, D.C., and Harrison, S.C. (2005). Structure of an unliganded simian immunodeficiency virus gp120 core. Nature *433*, 834–841.

Corti, D., Langedijk, J.P., Hinz, A., Seaman, M.S., Vanzetta, F., Fernandez-Rodriguez, B.M., Silacci, C., Pinna, D., Jarrossay, D., Balla-Jhagjhoorsingh, S., et al. (2010). Analysis of memory B cell responses and isolation of novel monoclonal antibodies with neutralizing breadth from HIV-1-infected individuals. PLoS One *5*, e8805.

Cutalo, J.M., Deterding, L.J., and Tomer, K.B. (2004). Characterization of glycopeptides from HIV-I(SF2) gp120 by liquid chromatography mass spectrometry. J. Am. Soc. Mass Spectrom. *15*, 1545–1555.

Destito, G., Yeh, R., Rae, C.S., Finn, M.G., and Manchester, M. (2007). Folic acid-mediated targeting of cowpea mosaic virus particles to tumor cells. Chem. Biol. *14*, 1152–1162.

Dhillon, A.K., Donners, H., Pantophlet, R., Johnson, W.E., Decker, J.M., Shaw, G.M., Lee, F.H., Richman, D.D., Doms, R.W., Vanham, G., et al. (2007). Dissecting the neutralizing antibody specificities of broadly neutralizing sera from human immunodeficiency virus type 1-infected donors. J. Virol. *81*, 6548–6562.

Dudkin, V.Y., Orlova, M., Geng, X., Mandal, M., Olson, W.C., and Danishefsky, S.J. (2004). Toward fully synthetic carbohydrate-based HIV antigen design: on the critical role of bivalency. J. Am. Chem. Soc. *126*, 9560–9562.

Dunlop, D.C., Ulrich, A., Appelmelk, B.J., Burton, D.R., Dwek, R.A., Zitzmann, N., and Scanlan, C.N. (2008). Antigenic mimicry of the HIV envelope by AIDS-associated pathogens. AIDS *22*, 2214–2217.

Geng, X., Dudkin, V.Y., Mandal, M., and Danishefsky, S.J. (2004). In pursuit of carbohydrate-based HIV vaccines, part 2: the total synthesis of high-mannose-type gp120 fragments—evaluation of strategies directed to maximal convergence. Angew. Chem. Int. Ed. Engl. *43*, 2562–2565.

Gray, E.S., Taylor, N., Wycuff, D., Moore, P.L., Tomaras, G.D., Wibmer, C.K., Puren, A., DeCamp, A., Gilbert, P.B., Wood, B., et al. (2009). Antibody specificities associated with neutralization breadth in plasma from human immunodeficiency virus type 1 subtype C-infected blood donors. J. Virol. *83*, 8925–8937.

Hessell, A.J., Rakasz, E.G., Poignard, P., Hangartner, L., Landucci, G., Forthal, D.N., Koff, W.C., Watkins, D.I., and Burton, D.R. (2009). Broadly neutralizing human anti-HIV antibody 2G12 is effective in protection against mucosal SHIV challenge even at low serum neutralizing titers. PLoS Pathog. *5*, e1000433.

Hong, V., Presolski, S.I., Ma, C., and Finn, M.G. (2009). Analysis and optimization of copper-catalyzed azide-alkyne cycloaddition for bioconjugation. Angew. Chem. Int. Ed. Engl. *48*, 9879–9883.

Iacob, R.E., Perdivara, I., Przybylski, M., and Tomer, K.B. (2008). Mass spectrometric characterization of glycosylation of hepatitis C virus E2 envelope glycoprotein reveals extended microheterogeneity of N-glycans. J. Am. Soc. Mass Spectrom. *19*, 428–444.

Joao, H.C., and Dwek, R.A. (1993). Effects of glycosylation on protein structure and dynamics in ribonuclease B and some of its individual glycoforms. Eur. J. Biochem. *218*, 239–244.

Joyce, J.G., Krauss, I.J., Song, H.C., Opalka, D.W., Grimm, K.M., Nahas, D.D., Esser, M.T., Hrin, R., Feng, M., Dudkin, V.Y., et al. (2008). An oligosaccharide-based HIV-1 2G12 mimotope vaccine induces carbohydrate-specific antibodies that fail to neutralize HIV-1 virions. Proc. Natl. Acad. Sci. USA *105*, 15684–15689.

Kaltgrad, E., Sen Gupta, S., Punna, S., Huang, C.-Y., Chang, A., Wong, C.-H., Finn, M.G., and Blixt, O. (2007). Anti-carbohydrate antibodies elicited by polyvalent display on a viral scaffold. ChemBioChem *8*, 1455–1462.

Kaltgrad, E., O'Reilly, M.K., Liao, L., Han, S., Paulson, J., and Finn, M.G. (2008). On-virus construction of polyvalent glycan ligands for cell-surface receptors. J. Am. Chem. Soc. *130*, 4578–4579.

Kozlovska, T.M., Cielens, I., Vasiljeva, I., Strelnikova, A., Kazaks, A., Dislers, A., Dreilina, D., Ose, V., Gusars, I., and Pumpens, P. (1996). RNA phase Q β coat protein as a carrier for foreign epitopes. Intervirology *39*, 9–15.

Krauss, I.J., Joyce, J.G., Finnefrock, A.C., Song, H.C., Dudkin, V.Y., Geng, X., Warren, J.D., Chastain, M., Shiver, J.W., and Danishefsky, S.J. (2007). Fully synthetic carbohydrate HIV antigens designed on the logic of the 2G12 antibody. J. Am. Chem. Soc. *129*, 11042–11044.

Kwong, P.D., Wyatt, R., Robinson, J., Sweet, R.W., Sodroski, J., and Hendrickson, W.A. (1998). Structure of an HIV gp120 envelope glycoprotein in complex with the CD4 receptor and a neutralizing human antibody. Nature *393*, 648–659.

Lee, H.K., Scanlan, C.N., Huang, C.Y., Chang, A.Y., Calarese, D.A., Dwek, R.A., Rudd, P.M., Burton, D.R., Wilson, I.A., and Wong, C.H. (2004). Reactivity-based one-pot synthesis of oligomannoses: defining antigens recognized by 2G12, a broadly neutralizing anti-HIV-1 antibody. Angew. Chem. Int. Ed. Engl. *43*, 1000–1003.

Lewis, W.G., Magallon, F.G., Fokin, V.V., and Finn, M.G. (2004). Discovery and characterization of catalysts for azide-alkyne cycloaddition by fluorescence quenching. J. Am. Chem. Soc. *126*, 9152–9153.

Li, H., and Wang, L.X. (2004). Design and synthesis of a template-assembled oligomannose cluster as an epitope mimic for human HIV-neutralizing antibody 2G12. Org. Biomol. Chem. *2*, 483–488.

Li, Y., Svehla, K., Louder, M.K., Wycuff, D., Phogat, S., Tang, M., Migueles, S.A., Wu, X., Phogat, A., Shaw, G.M., et al. (2009). Analysis of neutralization specificities in polyclonal sera derived from human immunodeficiency virus type 1-infected individuals. J. Virol. *83*, 1045–1059.

Liljas, L., and Golmohammadi, R. (1996). The crystal structure of bacteriophage Q β at 3.5 Å resolution. Structure *4*, 543–554.

Lin, T., Porta, C., Lomonossoff, G., and Johnson, J.E. (1996). Structure-based design of peptide presentation on a viral surface: the crystal structure of a plant/animal virus chimera at 2.8 Å resolution. Fold. Des. *1*, 179–187.

Lin, T., Chen, Z., Usha, R., Stauffacher, C.V., Dai, J.-B., Schmidt, T., and Johnson, J.E. (1999). The refined crystal structure of cowpea mosaic virus at 2.8 Å resolution. Virology *265*, 20–34.

Lomonossoff, G.P., and Hamilton, W.D.O. (1999). Cowpea mosaic virus-based vaccines. Curr. Top. Microbiol. Immunol. *240*, 177–189.

Luallen, R.J., Lin, J., Fu, H., Cai, K.K., Agrawal, C., Mboudjeka, I., Lee, F.H., Montefiori, D., Smith, D.F., Doms, R.W., et al. (2008). An engineered *Saccharomyces cerevisiae* strain binds the broadly neutralizing human immunodeficiency virus type 1 antibody 2G12 and elicits mannose-specific gp120-binding antibodies. J. Virol. *82*, 6447–6457.

Mascola, J.R., Stiegler, G., VanCott, T.C., Katinger, H., Carpenter, C.B., Hanson, C.E., Beary, H., Hayes, D., Frankel, S.S., Birx, D.L., et al. (2000). Protection of macaques against vaginal transmission of a pathogenic HIV-1/SIV chimeric virus by passive infusion of neutralizing antibodies. Nat. Med. *6*, 207–210.

Mehandru, S., Vcelar, B., Wrin, T., Stiegler, G., Joos, B., Mohri, H., Boden, D., Galovich, J., Tenner-Racz, K., Racz, P., et al. (2007). Adjunctive passive immunotherapy in human immunodeficiency virus type 1-infected individuals treated with antiviral therapy during acute and early infection. J. Virol. *81*, 11016–11031.

Miermont, A., Barnhill, H., Strable, E., Lu, X., Wall, K.A., Wang, Q., Finn, M.G., and Huang, X. (2008). Cowpea mosaic virus capsid, a promising carrier towards the development of carbohydrate based anti-tumor vaccines. Chem. Eur. J. *14*, 4939–4947.

Ni, J., Song, H., Wang, Y., Stamatos, N.M., and Wang, L.X. (2006). Toward a carbohydrate-based HIV-1 vaccine: synthesis and immunological studies of oligomannose-containing glycoconjugates. Bioconjug. Chem. *17*, 493–500.

Prasuhn, D.E., Jr., Yeh, R.M., Obenaus, A., Manchester, M., and Finn, M.G. (2007). Viral MRI contrast agents: coordination of Gd by native virions and attachment of Gd complexes by azide-alkyne cycloaddition. Chem. Commun. (Camb), 1269–1271.

Prasuhn, D.E., Jr., Singh, P., Strable, E., Brown, S., Manchester, M., and Finn, M.G. (2008). Plasma clearance of bacteriophage Qβ particles as a function of surface charge. J. Am. Chem. Soc. *130*, 1328–1334.

Rostovtsev, V.V., Green, L.G., Fokin, V.V., and Sharpless, K.B. (2002). A stepwise Huisgen cycloaddition process: copper(I)-catalyzed regioselective ligation of azides and terminal alkynes. Angew. Chem. Int. Ed. Engl. *41*, 2596–2599.

Sanders, R.W., Venturi, M., Schiffner, L., Kalyanaraman, R., Katinger, H., Lloyd, K.O., Kwong, P.D., and Moore, J.P. (2002). The mannose-dependent epitope for neutralizing antibody 2G12 on human immunodeficiency virus type 1 glycoprotein gp120. J. Virol. *76*, 7293–7305.

Scanlan, C.N., Pantophlet, R., Wormald, M.R., Ollmann Saphire, E., Stanfield, R., Wilson, I.A., Katinger, H., Dwek, R.A., Rudd, P.M., and Burton, D.R. (2002). The broadly neutralizing anti-human immunodeficiency virus type 1 antibody 2G12 recognizes a cluster of α1→2 mannose residues on the outer face of gp120. J. Virol. *76*, 7306–7321.

Scanlan, C.N., Pantophlet, R., Wormald, M.R., Saphire, E.O., Calarese, D., Stanfield, R., Wilson, I.A., Katinger, H., Dwek, R.A., Burton, D.R., et al. (2003). The carbohydrate epitope of the neutralizing anti-HIV-1 antibody 2G12. Adv. Exp. Med. Biol. *535*, 205–218.

Scanlan, C.N., Ritchie, G.E., Baruah, K., Crispin, M., Harvey, D.J., Singer, B.B., Lucka, L., Wormald, M.R., Wentworth, P., Jr., Zitzmann, N., et al. (2007). Inhibition of mammalian glycan biosynthesis produces non-self antigens for a broadly neutralising, HIV-1 specific antibody. J. Mol. Biol. *372*, 16–22.

Sen Gupta, S., Kuzelka, J., Singh, P., Lewis, W.G., Manchester, M., and Finn, M.G. (2005). Accelerated bioorthogonal conjugation: a practical method for the ligation of diverse functional molecules to a polyvalent virus scaffold. Bioconjug. Chem. *16*, 1572–1579.

Shenoy, S.R., Barrientos, L.G., Ratner, D.M., O'Keefe, B.R., Seeberger, P.H., Gronenborn, A.M., and Boyd, M.R. (2002). Multisite and multivalent binding between cyanovirin-N and branched oligomannosides: calorimetric and NMR characterization. Chem. Biol. *9*, 1109–1118.

Stamatatos, L., Morris, L., Burton, D.R., and Mascola, J.R. (2009). Neutralizing antibodies generated during natural HIV-1 infection: good news for an HIV-1 vaccine? Nat. Med. *15*, 866–870.

Strable, E., Prasuhn, D.E., Jr., Udit, A.K., Brown, S., Link, A.J., Ngo, J.T., Lander, G., Quispe, J., Potter, C.S., Carragher, B., et al. (2008). Unnatural amino acid incorporation into virus-like particles. Bioconjug. Chem. *19*, 866–875.

Trkola, A., Pomales, A.B., Yuan, H., Korber, B., Maddon, P.J., Allaway, G.P., Katinger, H., Barbas, C.F. III, Burton, D.R., Ho, D.D., et al. (1995). Cross-clade neutralization of primary isolates of human immunodeficiency virus type 1 by human monoclonal antibodies and tetrameric CD4-IgG. J. Virol. *69*, 6609–6617.

Trkola, A., Purtscher, M., Muster, T., Ballaun, C., Buchacher, A., Sullivan, N., Srinivasan, K., Sodroski, J., Moore, J.P., and Katinger, H. (1996). Human monoclonal antibody 2G12 defines a distinctive neutralization epitope on the gp120 glycoprotein of human immunodeficiency virus type 1. J. Virol. *70*, 1100–1108.

Trkola, A., Kuster, H., Rusert, P., Joos, B., Fischer, M., Leemann, C., Manrique, A., Huber, M., Rehr, M., Oxenius, A., et al. (2005). Delay of HIV-1 rebound after cessation of antiretroviral therapy through passive transfer of human neutralizing antibodies. Nat. Med. *11*, 615–622.

Virgin, H.W., and Walker, B.D. (2010). Immunology and the elusive AIDS vaccine. Nature *464*, 224–231.

Walker, L.M., Phogat, S.K., Chan-Hui, P.Y., Wagner, D., Phung, P., Goss, J.L., Wrin, T., Simek, M.D., Fling, S., Mitcham, J.L., et al. (2009). Broad and potent neutralizing antibodies from an African donor reveal a new HIV-1 vaccine target. Science *326*, 285–289.

Wang, L.X. (2006). Toward oligosaccharide- and glycopeptide-based HIV vaccines. Curr. Opin. Drug Discov. Devel. *9*, 194–206.

Wang, Q., Lin, T., Tang, L., Johnson, J.E., and Finn, M.G. (2002). Icosahedral virus particles as addressable nanoscale building blocks. Angew. Chem. Int. Ed. Engl. *41*, 459–462.

Wang, L.X., Ni, J., Singh, S., and Li, H. (2004). Binding of high-mannose-type oligosaccharides and synthetic oligomannose clusters to human antibody 2G12: implications for HIV-1 vaccine design. Chem. Biol. *11*, 127–134.

Wang, J., Li, H., Zou, G., and Wang, L.X. (2007). Novel template-assembled oligosaccharide clusters as epitope mimics for HIV-neutralizing antibody 2G12. Design, synthesis, and antibody binding study. Org. Biomol. Chem. *5*, 1529–1540.

Wang, S.K., Liang, P.H., Astronomo, R.D., Hsu, T.L., Hsieh, S.L., Burton, D.R., and Wong, C.H. (2008). Targeting the carbohydrates on HIV-1: interaction of

oligomannose dendrons with human monoclonal antibody 2G12 and DC-SIGN. Proc. Natl. Acad. Sci. USA *105*, 3690–3695.

Woods, R.J., Pathiaseril, A., Wormald, M.R., Edge, C.J., and Dwek, R.A. (1998). The high degree of internal flexibility observed for an oligomannose oligosaccharide does not alter the overall topology of the molecule. Eur. J. Biochem. *258*, 372–386.

Wyatt, R., and Sodroski, J. (1998). The HIV-1 envelope glycoproteins: fusogens, antigens, and immunogens. Science *280*, 1884–1888.

Wyatt, R., Kwong, P.D., Desjardins, E., Sweet, R.W., Robinson, J., Hendrickson, W.A., and Sodroski, J.G. (1998). The antigenic structure of the HIV gp120 envelope glycoprotein. Nature *393*, 705–711.

Zwick, M.B., Labrijn, A.F., Wang, M., Spenlehauer, C., Saphire, E.O., Binley, J.M., Moore, J.P., Stiegler, G., Katinger, H., Burton, D.R., et al. (2001). Broadly neutralizing antibodies targeted to the membrane-proximal external region of human immunodeficiency virus type 1 glycoprotein gp41. J. Virol. *75*, 10892–10905.

